LDA MEASUREMENTS IN HIGH MACH NUMBER AXISYMMETRIC JET SHEAR LAYERS

Tong Feng, James J McGuirk
Dept. Of Aero. and Auto. Eng.,
Loughborough University,
Loughborough, Leicestershire LE11 3TU, UK
j.j.mcguirk@lboro.ac.uk.

ABSTRACT

An experimental survey has been undertaken to understand the behaviour of the annular mixing layer in the initial near-field region of axisymmetric jet development. High Mach number jets issuing from a convergent nozzle at Nozzle Pressure Ratios (NPR) from 1.68 to 3.0 were measured using LDA instrumentation. Detailed radial profile data are reported, particularly within the potential core region for mean velocity, turbulence rms and turbulent shear stress. Significant effects of NPR for supercritical jets were observed in the inviscid shock cell region, but profiles in the shear layer collapsed remarkably well. The growth rate of the annular shear layer over the potential core length was evaluated for a range of NPRs including underexpanded cases. A comparison of the compressibility-induced reduction in shear layer growth rate with planar shear layer data showed notable differences, with compressibility effects beginning earlier and being stronger than for planar shear layers.

INTRODUCTION AND BACKGROUND

The primary motivation behind the current work is the increased interest, in the last decade or so, in exploration of novel methods for control of spreading rate and enhanced mixing of aeroengine exhaust nozzle plumes. Recently attention has focused on methods to manipulate the jet/ambient shear layer behaviour after nozzle exit. For civil applications the design target is jet noise reduction (e.g. by means of nozzle trailing edge modifications such as chevrons or serrations: Saiyed et al, 2000), with the jet Nozzle Pressure Ratio (NPR = jet total pressure/ambient static pressure) being subcritical and jet Mach number high subsonic. Recent interest has also extended the range of NPR to supercritical values (Long, 2005), with underexpanded jets, supersonic Mach numbers, and additional shock cell noise. For military applications, supercritical and improperly expanded jets are common, with the design objective for shear layer manipulation now being low observability (IR signature reduction), often leading to much more aggressive manipulation devices, e.g. tabs (Feng and McGuirk, 2006).

Underpinning these engineering applications is a large body of fundamental work on the spreading behaviour of turbulent shear layers under conditions of high Reynolds and Mach numbers. Clearly there is a need to understand in detail the characteristics of the baseline jet/ambient shear layer for a range of practically occurring conditions if means for manipulating its behaviour to achieve desired design effects are to be identified effectively. Much of this fundamental research has been focused on planar shear layers, with the classical experimental data of Papamoschou and Roshko (1988) documenting the significant reduction in shear layer growth rate due to compressibility effects. This reduction was found to collapse best when characterised using the convective Mach number M_c, the Mach number in a frame of reference moving with the speed of the dominant instability waves in the shear layer. This experiment has since been repeated by many authors. The recent re-examination by Barone et al (2006) of 11 sets of experimental data has lead to a new recommended curve for the collapse of the shear layer spreading rate of compressible planar shear layers, replacing the often quoted 'Langley' curve as the target for CFD modelling efforts.

The practical importance of compressible shear layers has meant that this problem has become a standard test case for validation of CFD predictions of compressible flows, and attracted considerable interest from the turbulence modelling community. Initial efforts were concentrated on RANS modelling and followed the route of introduction of extra compressibility terms in the turbulence model equations. An additional compressible contribution to the turbulence dissipation rate was suggested by Sarkar et al (1991) and Zeman (1990), and used to predict compressible shear layers using both two-equation and second moment closure models (e.g. Sarkar and Lakshmanan, 1991 and El Baz and Launder, 1993). However, although models based on dilatational dissipation were calibrated to produce the correct growth rate reduction with M_c, DNS predictions by Vreman et al (1996) showed that the direct dilatational effects on dissipation and pressure terms were insignificant, and they suggested indirect compressibility modifications to the pressure-strain term were required to capture the spreading rate reduction effect physically correctly. This has been confirmed also in the DNS calculations of Pantano and Sarkar (2002). Efforts to develop such pressure-strain term modifications have been explored by Batten et al (1999) and Lejeune and Kourta (1997). Finally, LES modelling has recently been applied to compressible plane mixing layers by Le Ribault (2005). M_c values of 0.16, 0.5 and 1.1 were predicted, with the growth rate suppression measured experimentally being successfully captured. The simulations were relatively insensitive to the SGS model used, with suppression of the predicted time-averaged pressure–strain term (extracted from the LES) as M_c increased being

predicted well compared to the DNS results of Pantano and Sarkar (2002).

One aspect, which seems important in the engineering context described above, has, however, received rather little attention. This is the study of annular rather than planar shear layers. Whilst the initial region (~2 jet diameters) of a round jet shear layer will behave like a planar shear layer, this is less certain for the shear layer development length up to the end of the potential core (~5-6 jet diameters). DNS of an annular shear layer was carried out by Freund et al (2000), but this work applied a temporally developing shear layer approach, with streamwise periodic conditions, so this again is probably only relevant to the early part of annular shear layer development. The results showed annular and planar shear layers were very similar, but given the restriction mentioned, this is perhaps not surprising. Some annular shear layer results may be extracted from work on the potential core length of compressible free jets (Witze, 1974), where it was found that potential core length grew with increased jet Mach number. This is consistent with the convective Mach number influence measured in planar shear layers, but was not compared quantitatively. The first measurements of growth rate and turbulence properties in high speed jets were conducted by Lau et al (1979). It was again observed that high jet Mach numbers reduced annular shear layer growth rates, but no attempt was made to compare these with planar shear layer data. The work of Bellaud et al (1999) presented data in a properly expanded supersonic jet at M_j=2.5 in an outer stream at M=0.2 (implying M_c~0.9) and commented that the growth rate was similar to a planar shear layer at the same M_c, but no specific data on this were presented

Finally, most of the data mentioned above were taken under conditions of full expansion of the jet (properly designed con-di nozzles were used to expand to shock free supersonic jets for supercritical NPRs > 1.89). Only the study of Saddington et al (2004) has considered underexpanded jets, but problems with measured swirl velocities and high levels of unsteadiness in the jet exit profile make these data unsuitable. It is not clear the extent to which the inviscid shock phenomena in the jet core under these conditions might affect shear layer behaviour compared to the planar and properly expanded data.

Based on the analysis presented above, it was the objective of the present work to carry out an experimental investigation of high Mach number axisymmetric annular shear layers. A range of jet NPR covering values of practical interest were selected, including moderately underexpanded cases. Care was taken to ensure that the data were gathered under carefully controlled conditions that minimised nozzle exit boundary layer type changes. Detailed mean velocity and turbulence statistics were gathered so that the data can form a benchmark CFD validation test case. The data were also processed to allow direct quantitative comparison between planar and annular shear layer growth rate suppression. The following section outlines the experimental facility and instrumentation used in this work, followed by a section reporting and analysing the results, which are summarised in the final concluding section of the paper.

TEST FACILITY AND INSTRUMENTATION

Experiments were carried out using a High Pressure Nozzle Test Facility (HPNTF) for supersonic nozzle flow studies. A detailed description of the facility has been provided by Feng and McGuirk (2007). A 0.15m diameter air supply pipeline delivers high pressure (15 bar abs.) air into the HPNTF test cell. The supply line contains a control valve for coarse regulation of the pressure to ~5 bar. Within the test cell (Fig.1) a globe valve (E) isolates the rig from the supply pipe (G) if needed. The flow is split into two streams, one to supply a primary nozzle (A) and the other to supply a larger diameter co-axial secondary nozzle (if needed) via a branched delivery pipe (F), a plenum and a contraction (B). All data reported here are, however, for primary nozzle flow alone. Mass flow and pressure control are carried out using fine control valves (D for primary flow, H for secondary). These are computer controlled pneumatic valves, which are automatically adjusted to hold the Nozzle Pressure Ratio (NPR) to a constant value (typically 1.5-4) to an accuracy of ± 1% during blow-down testing when nozzle size and NPR require a mass flow rate >1.0 kg/s. The facility can also produce heated jets using a combustor (C) located downstream of the primary control valve. The data reported here are for unheated flow, i.e. jet fluid total temperature equal to ambient air temperature (278K). The horizontal jet from the nozzle is available for detailed plume characterisation in a test length of ~ 1.5m before entering a detuner for noise attenuation and exhaust.

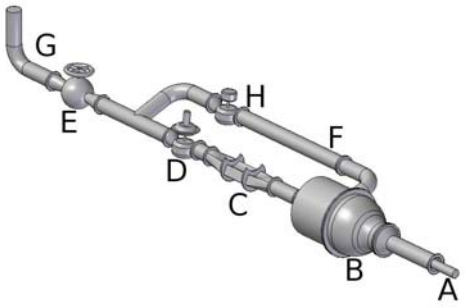

A	Primary nozzle delivery pipe
B	Secondary nozzle plenum/contraction
C	Combustion chamber
D	Primary nozzle control valve
E	Isolating globe valve
F	Secondary nozzle delivery pipe
G	Rig air supply pipe
H	Secondary nozzle control valve

Fig.1 High Pressure Nozzle Test Facility

.

Nozzle conditions were continuously logged on a PC in a separate control room. Typical blow-down times were between 15 to 30 mins. Colour Schlieren imaging and LDA measurements have been carried out. The colour Schlieren system used a red-green-blue combination; red indicating regions of expansion, blue compression regions, and green

corresponding to un-deflected light making up the neutral background. (NB only black and white images are presented here). Schlieren pictures were taken of the area just downstream of the nozzle exit (up to around $x/D_n \sim 5$). The LDA instrumentation (Fig.2) is a two-component fibre optic system manufactured by Dantec, made up of a 5W Argon Ion laser source, a beam transmitter, a beam projector, and a signal processor (BSA F80) specially designed for high speed flow measurement (maximum frequency ~80MHz, which with the optical arrangement used, corresponds to a velocity ~800 m/s). Seeding was provided either via liquid droplets, with an average size of 25µm and a specific weight of 0.912 g/cm^3, or solid alumina oxide particles with

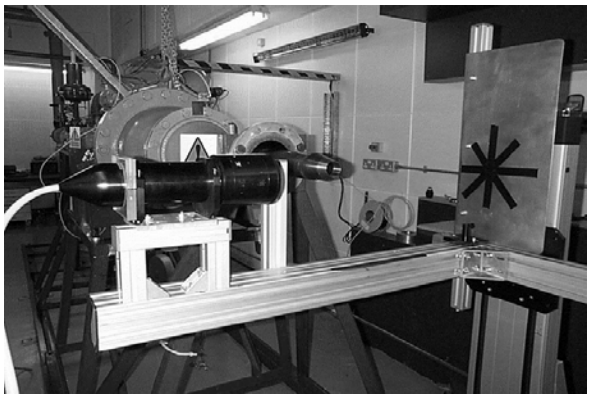

Fig.2 LDA system and traversing table

a diameter of 0.3µm and a density of 3.96 g/cm^3. Seeding was introduced at a location in the supply pipe 2.5m upstream of the nozzle to ensure the particles were fully mixed across the whole diameter. For underexpanded jets, due to condensation of the moisture in the ambient air entrained into the plume, it was not possible to use liquid seeding. The data rate achieved was typically 7~10KHz and a sample population of 20-50K validated readings were used to evaluate time-averaged statistics. The co-ordinate system used to present the data has the x-axis in the jet direction, the y-axis horizontal and the z-axis vertical. Measurements were carried out in the vertical x-z plane that passed through the nozzle exit centreline. To measure U and W velocity components, the optical axis of the laser beams was aligned horizontally (parallel to the y axis). The beam projector had a focal length of 310mm, beam spacing 38mm and beam diameter of 1.35mm, resulting in a measuring volume of 0.15mm in vertical and horizontal directions and 2.3mm along the optical axis). Traversing of the LDA probe across and along the jet plume was achieved using a three-axis Dantec traverse (see Fig. 2).

For tests in the HPNTF rig a conical convergent nozzle of exit diameter 48mm was used; this was provided with a short (~30mm) parallel extension to minimise any vena contracta effects. The nozzle dimensions are given in Fig 3. It has been noted in the work of Lepicovsky (1990) that the state of a nozzle exit boundary layer can change from laminar to transitional to turbulent as the jet NPR is varied. This can make quantitative assessment of jet spreading effects with NPR changes extremely difficult to identify. The recent work of Trumper (2007) has shown that this is due to the relaminarising effect of the favourable pressure gradient induced by the convergent nozzle. Trumper (2007)

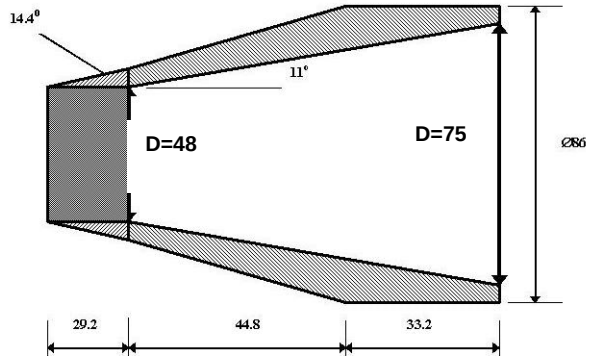

Fig. 3 Axisymmetric nozzle cross-section

also showed that the use of a short parallel nozzle extension provided the opportunity for a boundary layer, which had experienced strong relaminarisation on its passage through the nozzle, to relax back towards a fully turbulent state before reaching nozzle exit. The same approach has been followed here so that, under all conditions tested, the nozzle exit boundary layer is fully turbulent, with a momentum thickness Reynolds number O(4,000), as opposed to O(500) with no extension fitted.

RESULTS

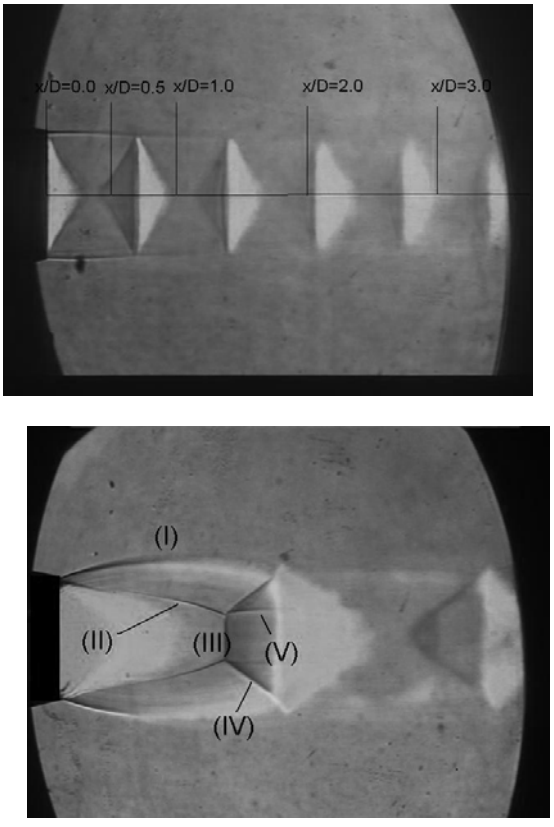

Fig. 4 Schlieren images
NPR = 2.32 (top), NPR = 6.0 (bottom)

Initial investigations used colour Schlieren imaging to examine flow structures. The presence of an inviscid repeated shock cell pattern in underexpanded jets is well known and is illustrated clearly in the images presented in Fig. 4. The top picture represents a moderately underexpanded case of NPR=2.32, showing the natural development of the jet and the expected pattern of repeated expansion and compression zones as the jet relaxes back to atmospheric pressure; only the first 5 shock cells are captured in the image. At the highest NPR tested (NPR=6.0, bottom picture), typical features of a strongly underexpanded jet are very well captured in the image: (I) highly curved jet/ambient plume boundary, (II) incident (or inception) shock, (III) Mach disc, (IV) conical reflected shock, (V) slip lines on the edges of the subsonic zone downstream of the Mach disc.

LDA data were gathered for a range of NPR (1.68-3.0) to cover both sub- and supercritical regimes. Fig. 5 shows measured mean velocity along the jet centreline, which clearly distinguishes the potential core behaviour for critical

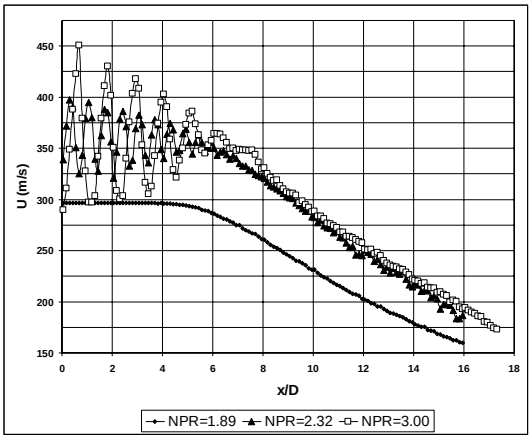

Fig. 5 Axial mean velocity on jet centreline

NPR (1.89 just choked), with constant centreline velocity, from the two supercritical underexpanded cases, with embedded shock cells and an oscillating centreline velocity. The amplitude of oscillation increases with NPR, but, as seen in Fig. 5, the number of shock cells decreases, 9 cells for NPR=2.32 but 5 cells for NPR=3. The measured data show good spatial resolution of the shock structure, but it must be noted that the seeding particle lag on passing through the oblique shocks will have smeared this somewhat. A Stokes law analysis to assess this was carried out, leading to the usual exponentially decaying lag between seed particles and fluid particles. Two particle response times ($\tau = \rho_p d_p^2/18\mu$) are needed to reduce the error between particle and fluid velocity to less than 10%. For a sudden change in gas velocity from 300m/s down to zero, this analysis implies that the particle relaxation time (2τ) is estimated as 0.26μs for liquid seeding and 1.1μs for the solid particles. The relaxation length before the seed particle is again following the flow faithfully is estimated as 0.25mm (liquid) and 1.09mm (solid), so smearing of this order of magnitude in the measured shock oscillations can be expected. It follows that it would be better to use liquid particle seeing, but, as noted above, due to moisture condensation, this was only possible in the very near nozzle exit for higher NPRs. A comparison of data taken for x/D<1.0 at the NPR=3 condition showed that, in the inviscid core, the measured velocity with solid particles in accelerating regions was always ~7% less than with liquid seeding. Fortunately, however, in the shear layer region of most interest here, there was less than 1% difference in measured mean velocity, and the turbulence correlations were also only marginally affected. Finally, note that in the fully merged jet downstream of x/D~10, there is no influence of NPR on the centreline decay rate.

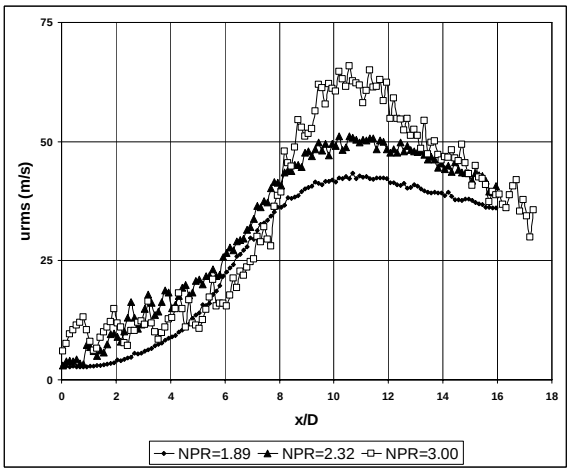

Fig. 6 Axial turbulence rms on jet centreline

Fig. 6 shows the development of the axial turbulence rms along the centreline for the same 3 NPRs. Three zones can be identified in the potential core region, most clearly in the lowest NPR, but on close inspection for all NPRs. For 0<x/D<2, the turbulence level remains close to that at nozzle exit, for 2<x/D<5 (i.e. still before potential core end) the turbulence rises but at a shallower gradient compared to the 3rd zone, after potential core end at x/D ~ 5. The rise in turbulence rms after x/D~5 is clearly due to the annular shear layer growing to meet the centreline, i.e. this is true shear generated turbulence. Before this the LDA measured velocity fluctuations are not shear generated turbulence but irrotational fluctuations caused by pressure fluctuations in the potential core due to the fluctuating inner edge of the annular shear layer. The oscillation sin the two higher NPR results are connected to the chock cell locations, but these are more likely to be due to the seed particle dynamics on passing through embedded pressure waves as discussed above than shock generated turbulence. The peak turbulence location is sensibly independent of NPR (~x/D=10), and the peak level, non-dimensionalised by the local centreline axial velocity (U_c), is similar for the two lower NPRs at ~14%, but slightly higher for NPR=3 at 16.5%; by x/D~16 the turbulence level is similar for all NPRs.

Non-dimensional radial profiles (scaled by U_c) at two axial locations (x/D= 0.5 and 4) are shown in Figs. 7-9 for mean axial velocity, axial rms and turbulent shear stress respectively, for all 3 NPRs. Whilst there are obviously small differences near the centreline caused by fixed x/D axial locations being in different regions of the expansion/compression waves as the shock cell length alters

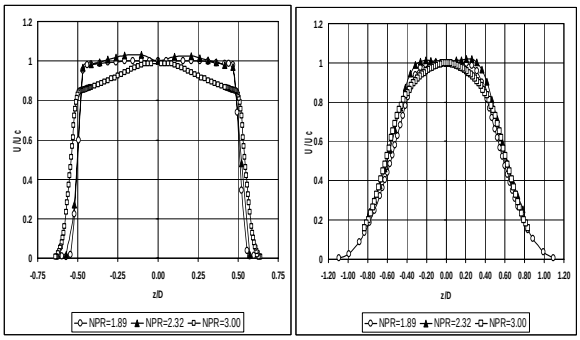

Fig. 7 Axial mean velocity radial profiles

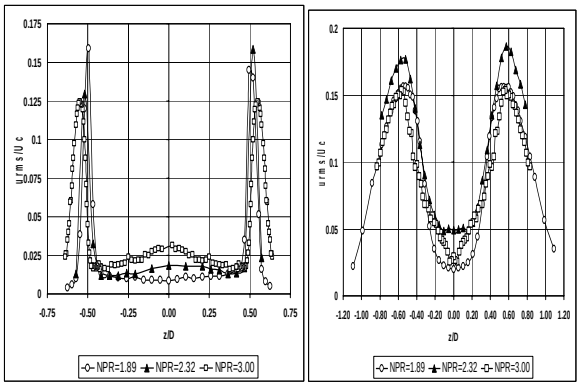

Fig. 8 Axial turbulence rms radial profiles

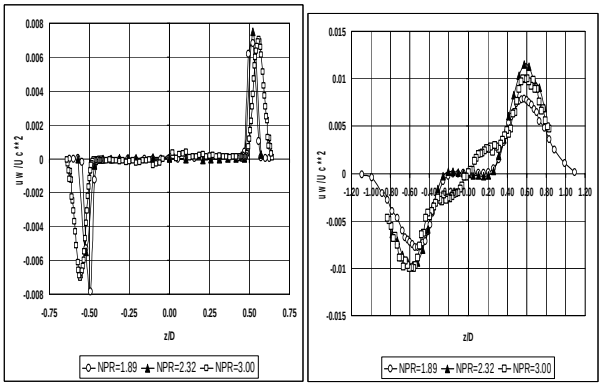

Fig. 9 Turbulent shear stress radial profiles

with NPR, in the shear layer region the non-dimensional profiles are remarkably similar at all NPRs. The highest NPR has its shear layer zone shifted radially outward compared to the other two cases, and this is due to the curvature of the jet/ambient boundary as NPR increases (seen in Fig. 4 although at an even higher NPR).

Radial profiles such as those shown in Figs. 7-9 were measured at 10 axial stations in the region 0<x/D<16 and for 6 subcritical and 8 supercritical (underexpanded) NPRs. The thickness of the mixing layer δ was evaluated following the definition of Brown and Roshko (1974), i.e. $\delta = U_c / \left[\partial U / \partial r\right]_{\max}$, where both local centreline velocity and maximum gradient were evaluated from the radial profiles. Graphs of the development of δ with axial distance then allowed accurate determination of the annular shear layer growth rate over the potential core length of the jet. Fig. 10 illustrates this for an underexpanded jet at NPR=2.32. Note that an accurate linear gradient could be evaluated for all NPRs. By non-dimensionalising this growth rate by the incompressible value (i.e. δ'/δ'_o), where

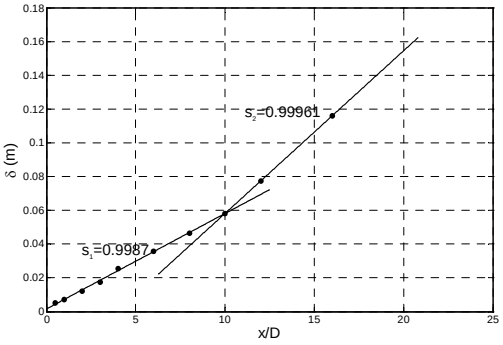

Fig. 10 Annular shear layer growth rate evaluation

$\delta_0^{'}$ = 0.166, and evaluating also the relevant convective Mach number M_c for each test condition, data for the current annular shear layers could be entered on a classical compressibility factor plot including also the latest planar shear layer evaluation of Barone et al (2006). (NB for underexpanded cases the availability of the measured axial velocity on the centreline allowed the local static temperature to be evaluated from an adiabatic gas dynamic energy equation and hence enabled the local speed of sound to be calculated). Fig. 11 shows the resulting comparison.

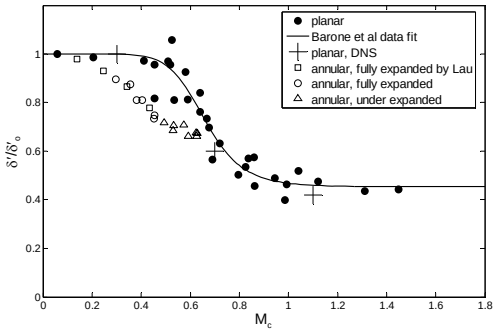

Fig. 11 Compressibility factor - shear layer growth rate

It is clear from this figure that annular shear layer data and planar shear layer data do not seem to collapse. The present experiments and the experiments of Lau et al (1979), both carried out using non-intrusive instrumentation in axisymmetric jets, agree well. The onset of compressibility reduction in growth rate seems to begin earlier in the annular shear layer data of Lau and the present work compared to planar shear layer data, although there is still some scatter in this. At similar values of convective Mach No. the present data indicate that annular growth rates are suppressed more than in the equivalent planar shear layer, at least for M_c values up to ~0.6. Underexpanded jets deviate

from the annular curve slightly. Experiments using a convergent nozzle cannot effectively produce higher M_c. Whilst the present study has confirmed that early data of Lau on compressibility effects in annular shear layers as being different to classical planar case, more experiments (with con-di nozzles and properly expanded supersonic jets) are needed to examine what happens at high M_c.

SUMMARY AND CONCLUSIONS

The present paper has reported on an experimental study of the axisymmetric annular shear layer behaviour associated with convergent nozzle jet plumes over a range of NPR, including moderately underexpanded cases. Detailed LDA measurements were taken with good axial and radial spatial resolution of both mean and turbulence properties. A few profiles were presented to illustrate what is believed to be a comprehensive database of measurements suitable for CFD validation. Post processing of the data allowed annular shear layer characteristics to be compared with planar shear layer data from the literature, specifically in terms of the reduction in shear layer growth rate caused by compressibility. The present data are in good agreement with the only other experimental survey of annular shear layers. The indication is that compressibility effects in annular shear layers begin at a lower convective Mach number and display stronger growth rate reduction than for planar shear layers. More experiments are required to confirm this, particularly at higher M_c.

ACKNOWLEDGEMENTS

This work was funded by EPSRC (Grant No GR/S27467/01) via the MSTTAR DARPS consortium.

REFERENCES

Barone, M. F., Oberkampf, W. L., Blottner, F. G., 2006, "Validation case study: prediction of compressible turbulent mixing layer growth rate", *AIAA Jnl*, Vol 44, pp 1488-1497.

Batten, P., Craft, T. J., Leschziner, M. A. L., Loyau, H., 1999, "Reynolds stress transport modelling for compressible aerodynamics applications", *AIAA Jnl*, Vol. 37, pp 785-796.

Bellaud, S., Barre, S., Bonnet, J-P., 1999, "Experimental study of annular supersonic mixing layers: turbulent kinetic energy budget", *Proc. Of 1st TSFP Symposium*, Eds. Banerjee, S., Eaton, J.K.

Brown, G. L. and Roshko, A., 1974, "On density effects and large structures in turbulent mixing layers", *Jnl of Fluid Mech*, Vol. 64, pp 775-816.

El Baz, A. M. and Launder, B. E., 1993, "Second moment modelling of compressible mixing layers", *Engineering Turbulence Modelling and Measurements 2*, Eds. Rodi, W. A. and Martinelli, F., Elsevier Press.

Feng, T., and McGuirk, J. J., 2006, "LDA measurements of underexpanded jet flow from an axisymmetric nozzle with tabs", *3rd AIAA Flow Control Conf.*, AIAA–2006-3702

Feng, T., and McGuirk, J. J., 2007, "LDA measurements of heated and unheated underexpanded jets from axisymmetric convergent nozzles", *18th ISABE Conf.*, ISABE–2007-1322.

Freund, J. B., Lele, S. K., Moin, P., 2000, "Compressibility effects in a turbulent annular mixing layer, Part 1: turbulence and growth rate", *Jnl of Fluid Mech*, Vol. 421, pp 229-267.

Lau, J. C., Morris, P. J., Fisher, M. J., 1979, "Measurements in subsonic and supersonic free jets using a laser velocimeter", *Jnl of Fluid Mech*, Vol. 93, pp 1-27.

Lejeune, C. and Kourta, A., 1997, "Modelling of extra compressibility terms in high speed turbulent flows", *Proc. Of 11th TSF Symposium*, pp. P3.71-P3.76.

Le Ribault, C., 2005, "Large eddy simulation of compressible mixing layers", *International Journal of Dynamics of Fluids*, Vol. 1, pp. 87-111.

Lepicovsky, J., 1990, "Total temperature effects on centreline Mach number characteristics of free jets", *AIAA Jnl*, Vol. 27, pp 712-718.

Long, D. F., 2005, "Effect of nozzle geometry on turbofan shock cell noise at cruise", *43rd AIAA Aerospace Sciences Meeting*, AIAA-2005-998.

Pantano, C. and Sarkar, S., 2002, "A study of compressibility effects in the high-speed turbulent shear layer", *Jnl of Fluid Mech*, Vol. 451, pp. 329-371.

Papamoschou, D. and Roshko, A., 1988, "The compressible turbulent shear layer: an experimental study", *Jnl of Fluid Mech*, Vol. 197, pp. 453-477.

Saddington, A. J., Lawson, N. J., Knowles, K., 2004, "An experimental and numerical investigation of underexpanded turbulent jets", *The Aeronautical Jnl*, Vol 108, pp 145-151.

Saiyed, N. H., Bridges, J. E., Mikkelson, K., 2000, "Acoustics and thrust of separate flow exhaust nozzles with mixing devices for high bypass ratio engines", *8th AIAA/CEAS Aeroacoustics Conference*, AIAA-2000-1961.

Sarkar, S., Erlebacher, G., Hussaini, M. Y., Kreiss, H. O., 1991, "The analysis and modelling of dilatational terms in compressible turbulence", *Jnl of Fluid Mech*, Vol. 227, pp 473-493.

Sarkar, S. and Lakshmanan, B., 1991, "Application of a Reynolds stress turbulence model to the compressible mixing layer", *AIAA Jnl*, Vol. 29, pp 743-749.

Trumper, M. T., 2006, "A study of nozzle exit boundary layers in high speed jet flows", Ph. D Thesis, Loughborough University.

Vreman, A.W., Sandham, N. D., Luo, K. H., 1996, "Compressible mixing layer growth rate and turbulence characteristics", *Jnl of Fluid Mech.*, Vol. 320, pp. 235-258

Witze, P. D., 1974, "Centreline velocity decay of compressible free jets", *AIAA Jnl*, Vol. 12, pp 417-418.

Zeman, O., 1990, "Dilatational dissipation: the concept and application in modelling compressible mixing layers", *Physics of Fluids A*, Vol. 2, pp.178-188.